Easy induction of a ferroelectric fourfold monoclinic domain state from a tetragonal ferroelectric monodomain state in $PbZn_{1/3}Nb_{2/3}O_3$

A Lebon[1,2,3], H Dammak[1] and G Calvarin[1]

[1] Structures, Propriétés et Modélisation des Solides, UMR 8580, CNRS—Ecole Centrale Paris, Grande Voie des Vignes, 92295 Châtenay-Malabry Cedex, France
[2] Laboratoire de Physique des Collisions Électroniques et Atomiques, Université de Bretagne Occidentale, 6 avenue Le Gorgeu, 29285 Brest Cedex, France

E-mail: alexandre.lebon@univ-brest.fr

Abstract

We report a combined pyroelectric, dielectic and structural characterization of PZN single crystals in field cooling (FC) run along [001]. The pyroelectric current and the dielectric permittivity show a new characteristic temperature, at $T \approx 370$ K, related to a macroscopic competition between two induced ferroelectric tetragonal (T) and monoclinic (M) phases. The phase transition, which starts around $T_{C-R} = 385$ K, spreads over a large temperature range and some amount of T-phase is still observed at room temperature (RT). The M–T phase mixture, induced below T_{C-R}, is stable after field removal. According to a previous Raman scattering work, a fourfold symmetry of M-domains is proposed; the residual T-phase is stabilized by the coexistence of four symmetry-allowed M-domains arranged around [001]. Our results confirm that in a restricted temperature range ($T_{C-R} - 20$ K, $T_{C-R} + 20$ K) the free energy of the relaxor-ferroelectric PZN is almost independent of the direction of polarization and accordingly the material can switch from one polar order to the other.

1. Introduction

Research on lead-based relaxor-ferroelectrics has been renewed with the discovery of exceptionally large piezoelectric and electromechanical coefficients in solid solutions of $PbMg_{1/3}Nb_{2/3}O_3$ (PMN) or $PbZn_{1/3}Nb_{2/3}O_3$ (PZN) with $PbTiO_3$ (PT). These properties are enhanced for single crystals, poled along [001], whose composition is very close to the morphotropic phase boundary (MPB) between the rhombohedral (R) and tetragonal (T)

phases [1]. The experimental observation of an intermediate monoclinic (M) phase in PZN–
xPT compositions close to the MPB [2] and the prediction of a polarization rotation path
under an electric field [3] improved the understanding of the high piezoelectric response in
these materials.

Whereas PMN, the prototype relaxor, exhibits an electric field induced cubic (C) →
rhombohedral (R) phase transition [4], the isomorphous PZN, the parent compound of the
PZN–PT family, displays a spontaneous C → R phase transition [5]. A recent high-resolution
x-ray diffraction study on single crystals [6] has shown that this transition spreads over the
temperature range $T_{CR} = 385(5)$ K–$T_R = 330(5)$ K; the C-phase transforms progressively
into R-domains, of average size 60–70 nm along {111} directions, that do not grow as the
temperature is lowered [6]. A recent high-resolution synchrotron x-ray diffraction study
completes the former study and demonstrates that in the temperature range T_{CR}–T_R the
rhombohedral domains coexist with a lower symmetry phase [7]. Structural studies under
applied field are less investigated; we know from a previous report that poling along the polar
direction [111] transforms the polydomain state into a quasi-single domain R-phase [6]. In
addition, above T_{CR}, the application of a dc-bias along [001] results in the induction of a single
domain T-phase. The longitudinal strain S_{33} of the induced T-phase is higher than that of the
R induced phase at equal field [8].

The present paper reports pyroelectric, dielectric and structural characterizations of PZN
single crystals poled along [001], performed in field cooling (FC) run. It is shown that the
T-phase, induced above T_{C-R}, progressively transforms into a M-phase from around T_{C-R}.
However, an amount of T-phase is stabilized down to room temperature (RT). The induction
of such a state is obtained through a poling with very moderate magnitude of electric field. An
arrangement of M-domains in a macroscopic fourfold symmetry is proposed in conjunction
with former Raman scattering data.

2. Experimental details

PZN single crystals were grown and cut in the same way as in [9]. A platelet shape crystal
($3 \times 2 \times 0.5$ mm^3), cut along (100), and a rhombus shape crystal, cut along (001), (100)
and (110), were used for the electric and structural characterizations, respectively. Before
sputtering Au/Cr electrodes, the single crystals were polished and annealed at 450 °C to
remove residual stresses. The pyroelectric current and dielectric permittivity measurements
were performed with an HP4192A (Hewlett Packard) impedance analyser, with a cooling rate
of 1 K min^{-1} [10]. The x-ray diffraction diagrams were recorded in Bragg–Brentano geometry
with a high-resolution two-axis diffractometer, designed and built in the laboratory [11].
A graphite monochromator was used to select the Cu Kβ wavelength ($\lambda = 0.139\,223$ nm)
produced by a rotating anode (Rigaku). A relative angular precision better than 0.002° (2θ) is
achieved, owing to a photoelectric encoder connected to the rotation axis of the diffractometer.
Single crystals were fixed on a copper sample holder within a N$_2$ flow cryostat mounted upon
a HUBER goniometric head.

3. Results

Figure 1 displays the dependence on temperature of the pyroelectric current I and of the
integrated polarization P of PZN, measured in FC for three magnitudes of electric field (E)
applied along [001]. The dependence of I and P, above $T_{C-R} = 385(5)$ K, have previously
been interpreted [8] as a signature of a field induced C (paraelectric) → T (ferroelectric)
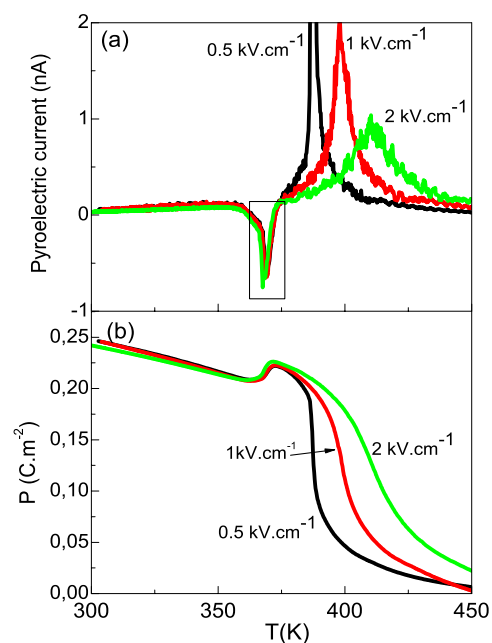
Figure 1. (a): Temperature dependence of the pyroelectric current of PZN, recorded in FC with a dc-electric field along [001], $E = 0.5$, 1.0 and 2.0 kV cm^{-1}; (b) derived macroscopic polarization.

(This figure is in colour only in the electronic version)
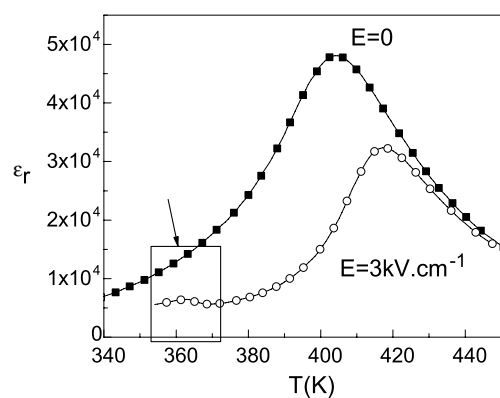
Figure 2. Temperature dependence of the dielectric permittivity of PZN performed in FC, at $f = 1$ kHz, with a dc-electric field parallel to [001]. The symbols (■), (O) correspond to the field magnitude $E = 0$ and 3.0 kV cm^{-1}, respectively.

phase transition, whose temperature increases with E. Below T_{C-R}, an additional small depolarization peak is measured at $T \approx 370$ K, a temperature which does not depend on E (figure 1(a)); at this temperature, the $P = f(T)$ curves show a pronounced down-turn (figure 1(b)).

Figure 2 shows the dependence on temperature of the real part of the dielectric permittivity of PZN, in zero FC ($E = 0$) and in FC ($E = 3$ kV cm^{-1}). A small increase of ε_r is observed in FC (see the rectangle in figure 2), in the same temperature range as for the pyroelectric current. This new characteristic temperature, evidenced by pyroelectric and dielectric measurements, prompted complementary structural studies under field applied along [001].

Three Bragg reflections, (004), (400) and (333), were investigated in the temperature range 420–340 K. For each temperature, three diagrams were successively recorded with $E = 0$, 4 and 0 kV cm^{-1} after $E = 4$ kV cm^{-1}. Between the two recorded series, the crystal was annealed at $T = 470$ K under zero field, in order to remove residual polarization. Figure 3 displays the diffraction peaks recorded at $T = 400$ and 360 K. At 400 K, the dependence
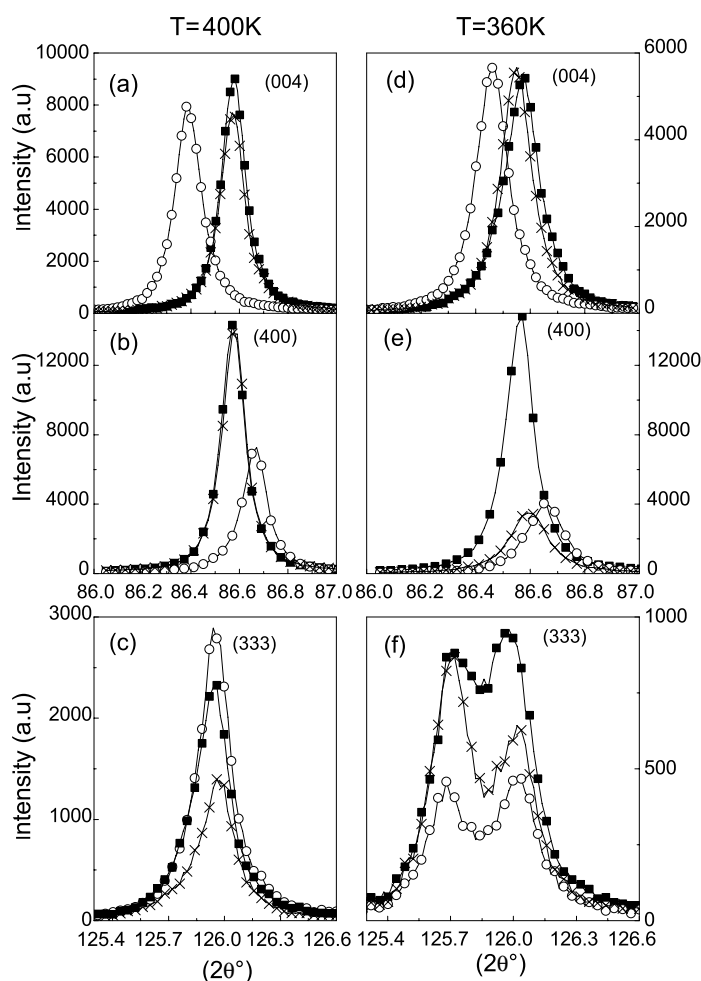
Figure 3. The Bragg reflections (004), (400) and (333) recorded at $T = 400$ K ((a), (b) and (c)) and $T = 360$ K ((d), (e) and (f)) under $E = 0$, and 4 kV cm^{-1} and $E = 0$ after $E = 4$ kV cm^{-1}. The symbol ■ stands for $E = 0$, ○ for $E = 4$ kV cm^{-1} and × stands for $E = 0$ after $E = 4$ kV cm^{-1}.

on E of the (004), (400) and (333) reflections was previously interpreted on the basis of a reversible C → T ferroelectric phase transition [8]. At $T = 360$ K and under zero field, PZN is characterized by nanometric R-domains embedded within a C-matrix [6]. Under $E = 4$ kV cm^{-1}, the (004) and (400) peaks are oppositely shifted, with respect to their angular position under $E = 0$ (figures 3(d) and (e)); this result is consistent with a T-symmetry but not with a R-symmetry. On the other hand, the permanence of two components for (333) (figure 3(f)) is consistent with a R-symmetry but not with a T-symmetry. After removal of the field, (004) and (400) exhibit a residual shift, about 0.015° for (004), and (333) still shows a doublet. As a remark, the diffraction peaks recorded under $E = 1$ kV cm^{-1}, not reported here, showed the same features but with smaller distortions. More importantly, the intensity collapses under $E = 4$ kV cm^{-1} of the (400) and (333) Bragg peaks, plotted respectively in figures 3(e) and (f), could result from a redistribution of the diffracted intensity in reciprocal space. To check this assumption, transverse scans (ω-scans at fixed 2θ) and longitudinal scans
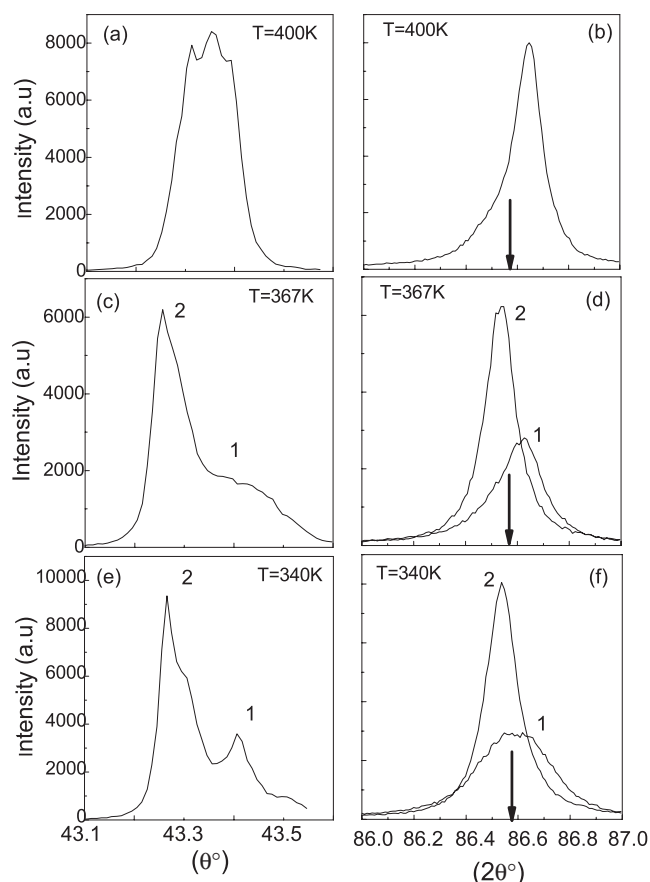
Figure 4. The (400) Bragg reflection recorded in FC ($E = 4$ kV cm^{-1}), at $T = 400$, 367 and 340 K. The left-hand diagrams (a), (c) and (e) are transverse ω-scans and the right-hand diagrams (b), (d) and (f) are the associated longitudinal ω–2θ scans; for these latter, an arrow indicates the position of the peak recorded without field.

(ω–2θ standard scans) of the (400) reflection were carried out in FC ($E = 4$ kV cm^{-1}) in the temperature range 420–300 K.

Figure 4 shows the transverse and the longitudinal scans of the (400) reflection, at three characteristic temperatures. At $T = 400$ K, the transverse scan (figure 4(a)) is characteristic of a slight crystal mosaic ($10'$) and the associated diffraction peak (figure 4(b)) is shifted towards higher angles, with respect to its position under $E = 0$ kV cm^{-1} (located by an arrow in figure 4(b)), in accordance with the induction of a T-phase. From about $T = 380$ K, the transverse scans show a broadening which becomes a clear splitting around $T = 370$ K, as it is shown in figure 4(c). The two diffraction peaks, associated to components 1 and 2 of the transverse scan, are displayed on figure 4(d). The Bragg angle ($2\theta_{max}$) of peak 1 is very close to the one of the T-phase at 400 K (figure 4(b)); on the other hand, peak 2 is shifted towards lower angles, which is indicative of a splitting of the (400) reflection in the plane normal to the field. At lower temperatures, the profile of the transverse scans still exhibits two components (figure 3(e)); the intensities of the associated diffraction peaks evolve with respect to each other down to $T = 340$ K, the intensity ratio of the two components is then constant from $T = 340$ K down to RT.
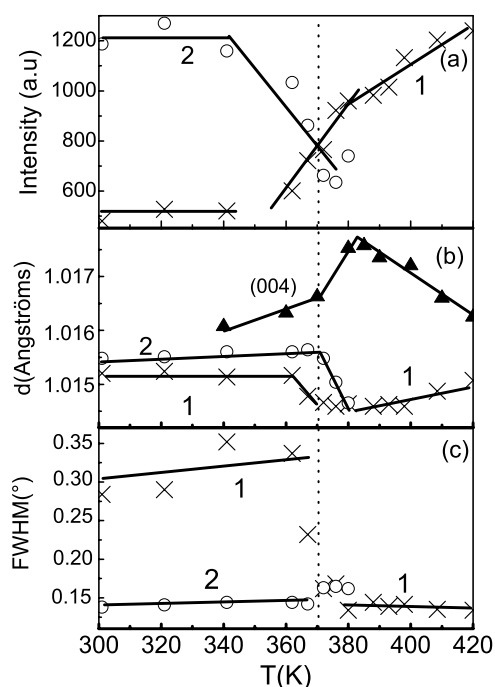
Figure 5. Temperature dependence of: intensities (a), interplanar spacings (b) and FWHM (c) of the two components of the (400) Bragg reflection, determined in FC ($E = 4$ kV cm^{-1}). The temperature dependence of the interplanar spacing of the (004) Bragg reflection is added on panel (b). 1 corresponds to the T phase and 2 to the incoming monoclinic phase. The dotted line emphasizes the temperature of the pyroelectric and dielectric anomalies. The black lines are guidelines for the eyes.

The temperature dependence of the integrated intensity I, of the interplanar spacing d and of the full width at half maximum (FWHM) of both (400) diffraction peaks 1 and 2 are shown in figure 5. The relative change of both $I = f(T)$ curves (figure 5(a)) is consistent with a phase transition, that starts at T_{C-R}, between the high-temperature T-phase (peak 1) and a new induced ferroelectric phase (peak 2). Just below T_{C-R}, the T-phase is predominant; as the temperature is lowered, the phase ratio (T/new phase) decreases and the crossover takes place at $T \approx 370$ K where the new phase becomes the majority phase. The phase mixture appears to be frozen from about $T = 340$ K. The FWHM of peak 2 (new phase) is quasi-invariable and is equal (0.14°) to that of peak 1 (T-phase) above T_{C-R} (figure 5(c)); on the other hand, in the temperature range where the T-phase is the minority phase ($T < 370$ K), its FWHM strongly increases up to $\approx$0.30°, reflecting a size or strain effect. Figure 5(b) plots the temperature dependence of d_{400} for both phases and the temperature dependence of d_{004} (interplanar spacing along the direction parallel to the field common to both phases). Above T_{C-R}, the dependence on T of d_{004} and d_{400} is in good agreement with results previously reported [8]. Below T_{C-R}, the interplanar spacing d_{004}, i.e. the cell parameter c common to both phases, decreases, whereas the interplanar spacings related to the components of the (400) increase and correlatively the cell parameters a of both phases. The sensitivity to dc-field application is maximum around T_{C-R}. The interplanar spacings d_{004} and d_{400} of the new phase are different (figure 5(c)); this result clearly rules out an R-symmetry but is consistent with an M-symmetry. The direction of the polar moment, with respect to the one of applied field (c-axis), is not accessible with our diffraction experiments. Therefore it is not possible to

discriminate between the two possible monoclinic space groups, Pm or Cm, which correspond to (e)–(d) and (e)–(f) paths, respectively, in the notation adopted by Fu and Cohen [3].

4. Discussion and conclusion

A T $\rightarrow$ M ferroelectric phase transition, induced under a field applied along [001], was evidenced in PZN from combined pyroelectric, dielectric and x-ray diffraction measurements. The transition, which starts around $T_{C-R} = 385$ K, spreads over a large temperature range and some amount of T-phase is still observed at RT. The temperature of depolarization peak and of the dielectric anomaly, $T \approx 370$ K, corresponds to an inversion of the T/M phase ratio determined by x-ray diffraction. When the field is removed after poling, (i) above T_{C-R}, the induced T-phase reversibly transforms into the C-phase; (ii) below T_{C-R}, the induced M– T phase mixture is irreversible, but the remnant distortion is weak if we compare it to the induction of the quasi-single domain state by the dc-field along [111] [6].

In a previous paper [13], we derived from the perfect loss of polarization of the Raman spectra recorded under field applied along [001], that the induced ferroelectric phase was made of domains arranged in a fourfold symmetry around [001]. This work proposes a monoclinic symmetry for these domains. Therefore, the stabilization of the T-phase down to RT can be explained by the coexistence of four symmetry-allowed M-domains arranged around [001], in the same way that for the spontaneous C $\rightarrow$ R phase transition for which a residual part of C-phase is stabilized by the coexistence of eight symmetry-allowed R-domains.

As a conclusion, our results show that a moderate field of 0.5 kV cm^{-1} is enough to induce the M-phase below T_{C-R}. It thus completes the study above T_{C-R} that demonstrates that a different kind of polar order could be induced by varying the direction of polarization above T_{C-R} [6, 7]. This confirms the flatness of the free energy [14] and the capability of lead-based relaxor-ferroelectrics to switch from one polar order to another depending of the poling direction and of the temperature range [8]. In this respect, it seems crucial to cross the temperature range of maximum distortion under field application, i.e. around T_{C-R}, to benefit from this characteristic of the relaxors. This physical feature allows a 'soft poling' of these materials as opposed to a 'hard poling' that is the application at RT of a very large dc-bias of typically $E = 40$ kV cm^{-1} [1, 12]; this idea has been fruitfully used for PZN–9% PT by Renault *et al* [15].

References

[1] Park S E and Shrout T R 1997 *J. Appl. Phys.* **82** 1804
[2] Noheda B, Cox D E, Shirane G, Park S-E, Cross L E and Zhong Z 2001 *Phys. Rev. Lett.* **86** 3891
[3] Fu H and Cohen R E 2000 *Nature* **403** 281
[4] Calvarin G, Husson E and Ye G 1995 *Ferroelectrics* **165** 349
[5] Yokomizo Y, Takahashi T and Nomura S 1970 *J. Phys. Soc. Japan* **28** 1278
[6] Lebon A, Dammak H, Calvarin G and Ahmedou I O 2002 *J. Phys.: Condens. Matter* **14** 7035
[7] Bing Y-H, Bokov A A, Ye Z-G, Noheda B and Shirane G 2003 *J. Phys.: Condens. Matter* **17** 2493
[8] Lebon A, Dammak H and Calvarin G 2003 *J. Phys.: Condens. Matter* **15** 3069
[9] Mulvihill M L, Park S E, Risch G, Li Z, Uchino K and Shrout T R 1996 *Japan. J. Appl. Phys.* I **35** 3984
　　Ahmedou I O 1997 *PhD Thesis* Ecole Centrale de Paris (in French)
[10] Dammak H, Renault A-E, Gaucher P, Thi M P and Calvarin G 2003 *Japan. J. Appl. Phys.* I **42** 6477
[11] Bérar J F, Calvarin G and Weigel D 1980 *J. Appl. Crystallogr.* **13** 201
[12] Lebon A, El Marssi M, Farhi R, Dammak H and Calvarin G 2001 *J. Appl. Phys.* **89** 3947
[13] Ishibashi Y and Iwada M 1999 *Japan. J. Appl. Phys.* **38** 1454
[14] Durbin M K, Hicks J C, Park S-E and Shrout T R 2000 *J. Appl. Phys.* **87** 8159
[15] Renault A-É, Dammak H, Calvarin G, Thi M P and Gaucher P 2002 *Japan. J. Appl. Phys.* **41** 3846